

## Secondary Structure Analysis of Individual Transmembrane Segments of the Nicotinic Acetylcholine Receptor by Circular Dichroism and Fourier Transform Infrared Spectroscopy\*

(Received for publication, September 19, 1997, and in revised form, October 28, 1997)

John Corbin‡, Nathalie Méthot§, Howard H. Wang‡, John E. Baenziger§, and Michael P. Blanton¶

From the ‡Department of Biology, University of California, Santa Cruz, California 95064, the §Department of Biochemistry University of Ottawa, Ottawa, Ontario K1H 8M5, Canada, and the ¶Department of Pharmacology, Texas Tech University Health Sciences Center, Lubbock, Texas 79430

Circular dichroism (CD) and attenuated total reflection Fourier transform infrared (ATR-FTIR) spectroscopy are used to establish the secondary structure of peptides containing one or more transmembrane segments (M1–M4) of the *Torpedo californica* nicotinic acetylcholine receptor (AChR). Peptides containing the M2–M3 and M1–M2–M3 transmembrane segments of the AChR  $\beta$ -subunit and the M4 segment of the  $\alpha$ - and  $\gamma$ -subunits were isolated from proteolytic digests of receptor subunits, purified, and reconstituted into lipid vesicles. For each peptide, an amide I vibrational frequency centered between 1650 and 1656  $\text{cm}^{-1}$  and negative CD absorption bands at 208 and 222 nm indicate that the peptide is largely  $\alpha$ -helical. In addition, the CD spectrum of a tryptic peptide of the  $\alpha$ -subunit containing the M1 segment is also consistent with a largely  $\alpha$ -helical structure. However, secondary structure analysis of the  $\alpha$ -M1 CD spectrum indicates the presence of other structures, suggesting that the M1 segment may represent either a distorted  $\alpha$ -helix, likely the consequence of several proline residues, or may not be entirely  $\alpha$ -helical. Overall, these findings are consistent with studies that indicate that the transmembrane region of the AChR comprises predominantly, if not exclusively, membrane-spanning  $\alpha$ -helices.

The nicotinic acetylcholine receptor (AChR)<sup>1</sup> from the electric organ of *Torpedo californica* is a pentameric glycoprotein composed of four homologous, transmembrane subunits in a stoichiometry of  $\alpha_2\beta\gamma\delta$  (1, 2). Each of the subunits associate about a central axis to form a cation-selective ion channel (for recent reviews, see Refs. 3 and 4). The AChR is the best characterized member of a family of ligand-gated ion channels that includes the  $\gamma$ -aminobutyric acid type A, the glycine, and the 5-hydroxytryptamine (serotonin) receptors (recent reviews include Refs. 5–7).

\* This work was supported in part by National Institutes of Health NINDS Grant R29 NS35786. The costs of publication of this article were defrayed in part by the payment of page charges. This article must therefore be hereby marked "advertisement" in accordance with 18 U.S.C. Section 1734 solely to indicate this fact.

¶ To whom correspondence should be addressed: Dept. of Pharmacology, Texas Tech University Health Sciences Center, 3601 4th St., Lubbock, TX 79430. Tel.: 806-743-2425; Fax: 806-743-27447; E-mail: phrmpb@ttuhsc.edu.

<sup>1</sup> The abbreviations used are: AChR, nicotinic acetylcholine receptor; ATR, attenuated total reflectance; FTIR, Fourier transform infrared; CD, circular dichroism; [<sup>125</sup>I]TID, 3-trifluoromethyl-3-(*m*-[<sup>125</sup>I]iodophenyl) diazepam; PAGE, polyacrylamide gel electrophoresis; HPLC, high performance liquid chromatography; V8 protease, *S. aureus* V8 protease; Tricine, *N*-tris(hydroxymethyl)methylglycine.

In the postsynaptic membrane, about half of the mass of the AChR projects extracellularly beyond the lipid bilayer. This projection, which is made up of the hydrophilic, amino-terminal half of each AChR subunit, contains the agonist binding sites and sites of *N*-linked glycosylation, whereas about 30% of the AChR is within the bilayer and the remaining portion is in the cytoplasmic domain (8–10). Hydropathy profiles indicate that each subunit contains four hydrophobic segments 20–30 amino acids in length, designated M1–M4, that were proposed to be membrane-spanning  $\alpha$ -helices (11–14). Although the transmembrane disposition of each of these segments has been fairly well established (reviewed in Ref. 15), the nature of their secondary structure is at present controversial. Based on recent electron microscopy results (Refs. 10 and 16; 9-Å resolution), the transmembrane structure of the AChR is proposed to consist of a ring of five  $\alpha$ -helices surrounded by a rim of  $\beta$ -strands. The five helices, which are associated at the central axis, lining the pore of the ion channel, are presumed to be made up of M2 segments from each subunit, based upon results of photoaffinity labeling studies done with non-competitive antagonists and functional studies of AChRs with mutations within M2 (reviewed in Refs. 17 and 18). Since no additional  $\alpha$ -helices were apparent in the rim of electron density flanking the M2 helices, the remaining transmembrane structure, which would be made up of the M1, M3, and M4 hydrophobic segments, was assumed to be organized as  $\beta$ -sheets (see also Ref. 19).

In contrast, studies using several different photoactivatable hydrophobic probes have identified amino acid residues in contact with the lipid bilayer in the M3 and M4 segments of each of the AChR subunits (20–23); from the periodicity of labeled residues, it was concluded that each of these segments is organized as a transmembrane  $\alpha$ -helix. The structure of the AChR was also examined using a combination of hydrogen-deuterium exchange and FTIR spectroscopy (24). The presence of an exchange-resistant pool of  $\alpha$ -helical peptides was interpreted as providing evidence for a predominantly  $\alpha$ -helical secondary structure of the AChR transmembrane domains. The simplest interpretation of these studies is that the hydrophobic segments M1–M4 in each of the AChR subunits are organized as a bundle of four membrane-spanning  $\alpha$ -helices.

Determining the structure of individual transmembrane segments in each of the AChR subunit remains an important goal. This is particularly true if, as the former set of studies suggest, the AChR membrane-spanning domains comprise both  $\alpha$ -helical and  $\beta$ -sheet type structures. In the present study, we isolated peptides that contained one or more transmembrane segments of the AChR and determined the secondary structure of the lipid reconstituted peptide using both CD and FTIR spectroscopy. The largely  $\alpha$ -helical nature of each of these peptides

provides additional support for a model of the transmembrane region of the AChR that comprises membrane-spanning  $\alpha$ -helices.

#### EXPERIMENTAL PROCEDURES

**Materials**—*Staphylococcus aureus* V8 protease was purchased from ICN Biochemicals and L-1-tosylamido-2-phenylethyl chloromethyl ketone-treated trypsin from Worthington Biochemical Corp. Genapol C-100 (10%) was purchased from Calbiochem. Asolectin, a crude soybean lipid extract, was from Avanti Polar Lipids. Spectra/Por Dispo Dialyzers (molecular weight cut-off = 2000) were from Spectrum.

**AChR-rich Membranes**—AChR-rich membranes were isolated from the electric organ of *T. californica* (Aquatic Research Consultants, San Pedro, CA) according to the procedure of Sobel *et al.* (25) with the modifications described previously (26). The final membrane suspensions in 36% sucrose, 0.02% NaN<sub>3</sub> were stored at -80 °C under argon.

**Preparation of Proteolytic Fragments of AChR Subunits Which Contain One or More Transmembrane Segments**—AChR subunits were resolved by SDS-PAGE (27) using 1.5-mm-thick 8% polyacrylamide gels with 0.33% bis(acrylamide). Typically, 10–12 mg of AChR membranes were resolved on a single 1.5-mm gel, with 40–50 mg processed in a single experiment. Polypeptides were visualized by staining with Coomassie Blue R-250 (0.25% w/v in 45% methanol and 10% acetic acid) and destaining in 25% methanol, 10% acetic acid. Gels were soaked in distilled water overnight and individual AChR subunit bands excised. For the AChR  $\alpha$ -subunit, the excised gel pieces were transferred to the wells of individual 15% mapping gels (26, 28). The  $\alpha$ -subunit was proteolytically digested in the gel with *S. aureus* V8 protease and following staining and destaining the V8 fragments  $\alpha$ -V8-10 (Asn<sup>339</sup>-Gly<sup>437</sup>) and  $\alpha$ -V8-20 (Ser<sup>173</sup>-Glu<sup>338</sup>) were excised (21). AChR subunits and V8 proteolytic fragments were isolated from the excised gel pieces by passive elution (21, 29). The eluate was filtered and the protein concentrated using a Centrprep-10 (Amicon). Excess SDS was removed by acetone precipitation (overnight at -20 °C).

Receptor subunits,  $\alpha$ -V8-10, and  $\alpha$ -V8-20 were proteolytically digested and peptides purified using protocols similar to those reported previously (21). For trypsin digestion, acetone-precipitated AChR subunits and V8 protease fragments were resuspended in a small volume (~100  $\mu$ l) of buffer (100 mM NH<sub>4</sub>HCO<sub>3</sub>, 0.1% SDS, pH 7.8). The SDS concentration was then reduced by diluting with buffer without SDS, and Genapol C-100 (Calbiochem) was added, resulting in final concentrations of 0.02% SDS, 0.5% Genapol C-100, and 1–2 mg/ml protein. Trypsin was added up to a total of 1:5 (w/w) enzyme to substrate ratio for intact subunits (~1 mg of protein) and to 1:1 (w/w) for  $\alpha$ -V8-10 and  $\alpha$ -V8-20. The digests were incubated at room temperature for 3–4 days and the resulting peptides separated on 1.5-mm-thick small pore Tricine SDS-PAGE gels (30). Following staining and destaining of a strip of each Tricine gel, selected fragments were excised based upon previous results (21) and with the aid of prestained low molecular weight standards (Life Technologies, Inc.).

Isolated fragments were further purified by reverse-phase HPLC using a Brownlee Aquapore C<sub>4</sub> column (100  $\times$  2.1 mm). Solvent A was 0.08% trifluoroacetic acid in water, and Solvent B was 0.05% trifluoroacetic acid in 60% acetonitrile, 40% 2-propanol. The flow rate was maintained at 0.2 ml/min and 0.5-ml fractions collected. Prior to injection, material isolated from excised gel pieces was filtered, the protein concentrated using a Centricon-3 (Amicon), and the material then spun briefly (15,000 rpm for ~10 s) in a table-top microcentrifuge to sediment any insoluble material. Peptides were eluted with a nonlinear gradient from 25% to 100% Solvent B in 80 min. The elution of peptides was monitored by the absorbance at 210 nm.

Peptide containing HPLC fractions were pooled and dried by vacuum centrifugation. Peptides were resuspended in 1 ml of 2% octyl- $\beta$ -glucoside and asolectin lipid in 2% sodium cholate added to achieve an estimated lipid to peptide molar ratio of ~15:1. The octyl- $\beta$ -glucoside and sodium cholate were removed by dialysis using Spectra/Por CE Dispo Dialyzers (molecular weight cut-off, 2000) for 2 days against phosphate buffer (10 mM phosphate, 5 mM NaCl, pH 7.0). Each sample was concentrated to 200  $\mu$ l using a Centricon-3 and stored at -80 °C. A small aliquot of each sample was subjected to NH<sub>2</sub>-terminal amino acid sequence analysis to confirm the identity of the peptide and estimate its concentration. An additional aliquot was labeled with the hydrophobic photoreagent [<sup>125</sup>I]TID. The labeled peptide was resolved on a 1.0-mm-thick Tricine gel and the dried gel subjected to autoradiography. Labeling with [<sup>125</sup>I]TID served as an additional test of peptide purity and to confirm that no significant peptide aggregation (irreversible) had occurred.

**Circular Dichroism**—CD spectra were measured with a AVIV 60DS spectropolarimeter in a rectangular quartz cuvette of 0.1 cm path length. Repetitive scans (5–10 scans) were recorded and averaged at 25 °C with a 1-s integration time, a 0.1-nm step size, and a 1.5-nm bandwidth. The spectra were collected in phosphate buffer (10 mM phosphate, 5 mM NaCl, pH 7.0). The protein concentration in the samples was determined by NH<sub>2</sub>-terminal amino acid sequence analysis. Spectra of peptide-free lipid vesicles prepared in parallel with the lipid-peptide samples and were used to correct for background lipid absorbance and scattering. Secondary structure estimations were obtained by spectral deconvolution using the Prosec program (AVIV Instruments) using the four-basis spectra set ( $\alpha$ -helix,  $\beta$ -sheet,  $\beta$ -turn, and other) of Chang *et al.* (31).

**FTIR Spectroscopy**—FTIR spectra were acquired using the attenuated total reflectance (ATR) technique on an FTS-40 spectrometer equipped with a mercury cadmium telluride detector. The spectrometer was purged with dry air (dew point -100 °C) from a Balston air dryer (Balston, Haverhill, MA). FTIR spectra were obtained at a resolution of 2 cm<sup>-1</sup> with a minimum of 256 scans/spectrum. Samples were prepared by spreading an aliquot of the reconstituted peptide on the surface of a 50 mm  $\times$  20 mm  $\times$  2-mm germanium ATR crystal (Harrick, Ossining, NY). Bulk solvent was evaporated with a gentle stream of N<sub>2</sub> gas and the ATR crystal immediately installed in an ATR liquid sample cell. Evaporation of the bulk <sup>1</sup>H<sub>2</sub>O solution was required to obtain a protein signal of reasonable strength relative to the overlapping absorbance of <sup>1</sup>H<sub>2</sub>O. After data acquisition, samples were exposed to <sup>2</sup>H<sub>2</sub>O buffer (5 mM phosphate, 250 mM NaCl, 5 mM KCl, 2 mM MgCl<sub>2</sub>, 3 mM CaCl<sub>2</sub>, pH 6.6). The bulk solvent was evaporated by flowing N<sub>2</sub> gas through the ATR sample compartment, and spectra of the deuterated peptides were recorded.

Spectral deconvolution was performed using GRAMS/386 version 1 (Galactic Industries, Salem, NH) and a  $\gamma = 3.5$  and a smoothing factor of 0.2. Prior to deconvolution, all spectra were examined for the presence of water vapor as described by Reid and Baenziger (32).

**Sequence Analysis**—Amino-terminal sequence analysis was performed on a Beckman Instruments (Porton) model 20/20 protein sequencer using gas phase cycles (Texas Tech Biotechnology Core Facility). Peptide aliquots (~5–10  $\mu$ l) were immobilized on chemically modified glass fiber discs (Beckman Instruments), which were used to improve the sequencing yields of hydrophobic peptides (33). Peptides were subjected to 10 sequencing cycles and Initial yield (*I*<sub>n</sub>) and repetitive yield (*R*) were calculated by nonlinear least squares regression of the observed release (*M*) for each cycle (*n*):  $M = I_n R^n$  (phenylthiohydantoin-derivatives of Ser, Thr, Cys, and His were omitted from the fit).

#### RESULTS

**Isolation and Reconstitution of Proteolytic Fragments Containing AChR Transmembrane Segments**—Peptides containing the transmembrane segments M2-M3 (Met<sup>249</sup>-Arg<sup>307</sup>), M1-M2-M3 (Lys<sup>216</sup>-Arg<sup>307</sup>) of the AChR  $\beta$ -subunit, the M4 segment of the  $\alpha$ - and  $\gamma$ -subunits (Tyr<sup>401</sup>-Gly<sup>437</sup>, Val<sup>446</sup>-Arg<sup>485</sup>, respectively), and the M1 segment (Ile<sup>210</sup>-Lys<sup>242</sup>) of the  $\alpha$ -subunit were isolated from proteolytic digests of receptor subunits. Subunit digests were resolved by Tricine SDS-PAGE, and bands corresponding to these selected fragments were excised on the basis on their known electrophoretic migration (20, 21, 34). Figs. 1 and 3A show the reverse-phase HPLC elution profile of each fragment. Peak HPLC fractions (*arrow*) were pooled, the solvent removed, the peptide resuspended in detergent (octyl- $\beta$ -glucoside), and reconstituted into asolectin (a crude soybean lipid extract) vesicles. The identity and concentration of each reconstituted peptide was assessed by NH<sub>2</sub>-terminal amino acid sequence analysis. For each peptide, any secondary sequences (peptides) that were detected were present at 1/10 to 1/20 the amount of the primary sequence. An aliquot of each peptide was labeled with the hydrophobic photoreagent [<sup>125</sup>I]TID and the labeled peptide resolved by Tricine SDS-PAGE. For each peptide, a single band was apparent in the corresponding autoradiograph and migrating with the appropriate apparent molecular weight. [<sup>125</sup>I]TID-labeled peptide also provided a means of verifying that the peptide had not undergone any significant (irreversible) aggregation.

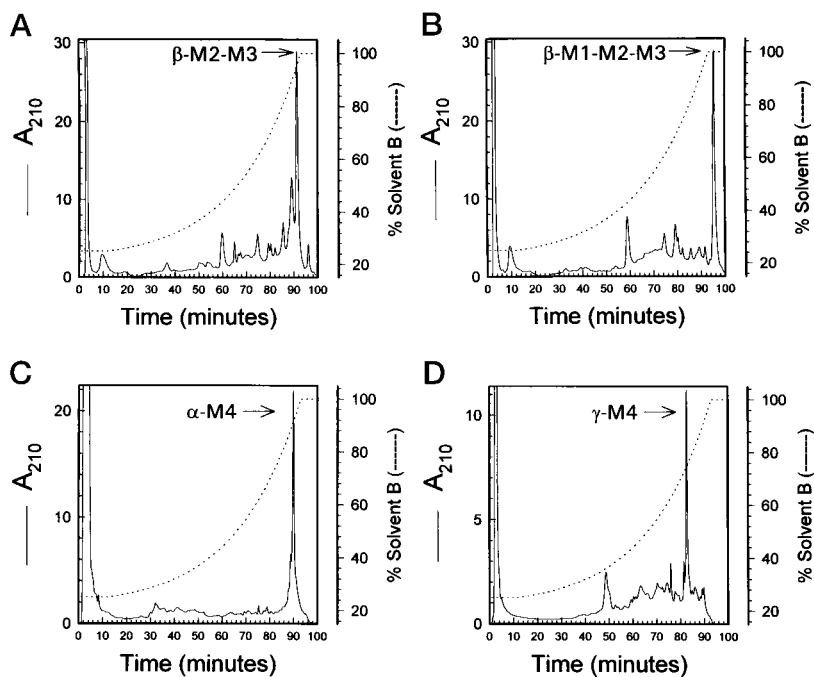


**FIG. 1. Reverse-phase HPLC purification of transmembrane fragments from tryptic digests of  $\alpha$ -V8-10 and the  $\beta$ - and  $\gamma$ -subunit.** AChR-rich membranes ( $\sim 50$  mg of protein) were resolved by SDS-PAGE and each of the AChR subunits isolated. For the  $\alpha$ -subunit,  $\alpha$ -V8-10 (Asn<sup>339</sup>-Gly<sup>437</sup>) was isolated from a limited "in gel" digest of the intact subunit (see "Experimental Procedures"). Receptor subunits as well as  $\alpha$ -V8-10 were then digested in solution with trypsin, and the digests resolved on 1.5-mm-thick 16.5% T, 6% C Tricine SDS-PAGE gels. Tryptic gel fragments  $\alpha$ -T-4K,  $\beta$ -T-10K,  $\beta$ -T-8K, and  $\gamma$ -T-5K were isolated from  $\alpha$ -V8-10,  $\beta$ -subunit, and  $\gamma$ -subunit, respectively. The fragments were then further purified by reverse-phase HPLC on a Brownlee Aquapore C4 column ( $100 \times 2.1$  mm); the elution gradient is shown by a dotted line (solvent A, 0.08% trifluoroacetic acid in water; solvent B, 0.05% trifluoroacetic acid in 60% acetonitrile, 40% 2-propanol). The elution of each peptide was monitored by absorbance at 210 nm (solid line). Panels A-D contain the HPLC elution profiles for gel fragments  $\beta$ -T-8K,  $\beta$ -T-10K,  $\alpha$ -T-4K, and  $\gamma$ -T-5K, respectively. In each panel, an arrow shows where each fragment elutes and the identity of each fragment was subsequently confirmed by NH<sub>2</sub>-terminal amino acid sequence analysis.

**CD Spectroscopy**—CD measurements provide a convenient method of looking at the overall secondary structure of a given protein or peptide, from which the relative contributions of different secondary structures can be estimated (35, 36). However, the CD spectra of membrane proteins is complicated by the fact that the spectra often exhibit various degrees of distortion in shapes, intensities, etc., that result from optical artifacts of differential light scattering and adsorption flattening (reviewed in Ref. 37). It is therefore important that secondary structure estimations be interpreted qualitatively.

Fig. 2 shows the CD spectra of peptides  $\beta$ -M2-M3,  $\beta$ -M1-M2-M3,  $\alpha$ -M4, and  $\gamma$ -M4 reconstituted into asolectin lipid vesicles (lipid:protein ratio,  $\sim 15:1$ ). In each sample, minima are observed at approximately 208 and 222 nm that are characteristic of  $\alpha$ -helical structure. Similar CD spectra (data not shown) were obtained for these same peptides reconstituted into octyl- $\beta$ -glucoside (2% w/v) or sodium dodecyl sulfate (10 mM) micelles. Micellar SDS is considered to be a good membrane-mimetic solvent (38, 39). For example, synthetic peptides of transmembrane segments of bacteriorhodopsin retain their  $\alpha$ -helical structure in SDS (40, 41). However, it should also be said that there exists considerable uncertainty about the accuracy of predicting the correct structure of a peptide in any single solvent environment (42). To qualitatively estimate the amount of peptide present in the  $\alpha$ -helical state, the CD spectra were deconvolved using the basis spectra of Chang *et al.* (31). The Chang *et al.* basis spectra were derived from linear analysis of the CD spectra from 16 globular proteins with high resolution crystal structures. The spectral deconvolution results are summarized in Table I. For each peptide,  $\alpha$ -helix was the predominant secondary structure conformation (e.g.  $\beta$ -M2-M3, 85%  $\alpha$ -helix, 15%  $\beta$ -turn).

Fig. 3B shows the CD spectrum of the reconstituted  $\alpha$ -M1

peptide (Ile<sup>210</sup>-Lys<sup>242</sup>). Although the spectrum exhibits minima at approximately 208 and 222 nm characteristic of  $\alpha$ -helical structure, the minimum at 208 nm is substantially reduced in magnitude. The results of spectral deconvolution (Table II) indicate that the peptide is largely  $\alpha$ -helical (56%) but that there is also a substantial amount of non-helical structure present (44%).

**ATR-FTIR Spectroscopy**—Representative FTIR spectra for the transmembrane peptide  $\gamma$ -M4 ( $\gamma$ -T-5K) recorded in both <sup>1</sup>H<sub>2</sub>O and <sup>2</sup>H<sub>2</sub>O are shown in Fig. 4, A and B, respectively. The amide I band (1600–1700 cm<sup>-1</sup>) is due predominantly to the stretching vibration of the peptide carbonyl, the frequency of which is highly sensitive to hydrogen bonding and thus protein secondary structure (43). In <sup>1</sup>H<sub>2</sub>O, the amide I band for  $\gamma$ -M4 is roughly symmetric with an intense peak maximum centered near 1656 cm<sup>-1</sup>. Two weak shoulders are also located near 1677 and 1627 cm<sup>-1</sup>. The spectral shape and peak maximum are both highly characteristic of peptides in an  $\alpha$ -helical conformation, which suggests that  $\gamma$ -M4 adopts a predominantly  $\alpha$ -helical secondary structure. However, peptides in a solvent exposed "random coil" conformation can also vibrate in the 1655 cm<sup>-1</sup> region in <sup>1</sup>H<sub>2</sub>O.

To distinguish between the contributions of  $\alpha$ -helical and random structures to the 1655 cm<sup>-1</sup> maximum, spectra were recorded after exposure of the nAChR to <sup>2</sup>H<sub>2</sub>O. The exchange of peptide hydrogens for deuterium leads to a shift in intensity from the 1656 cm<sup>-1</sup> down to both 1653 cm<sup>-1</sup> and roughly 1640 cm<sup>-1</sup>. The former shift in intensity from near 1656 cm<sup>-1</sup> down to 1653 cm<sup>-1</sup> is highly characteristic of the up to 5 cm<sup>-1</sup> downshifts in frequency that have been observed upon exposure of other  $\alpha$ -helical peptides to <sup>2</sup>H<sub>2</sub>O (24, 44). In contrast, the shift in frequency from near 1656 cm<sup>-1</sup> down to near 1640 cm<sup>-1</sup> is highly characteristic of the downshifts in frequency of

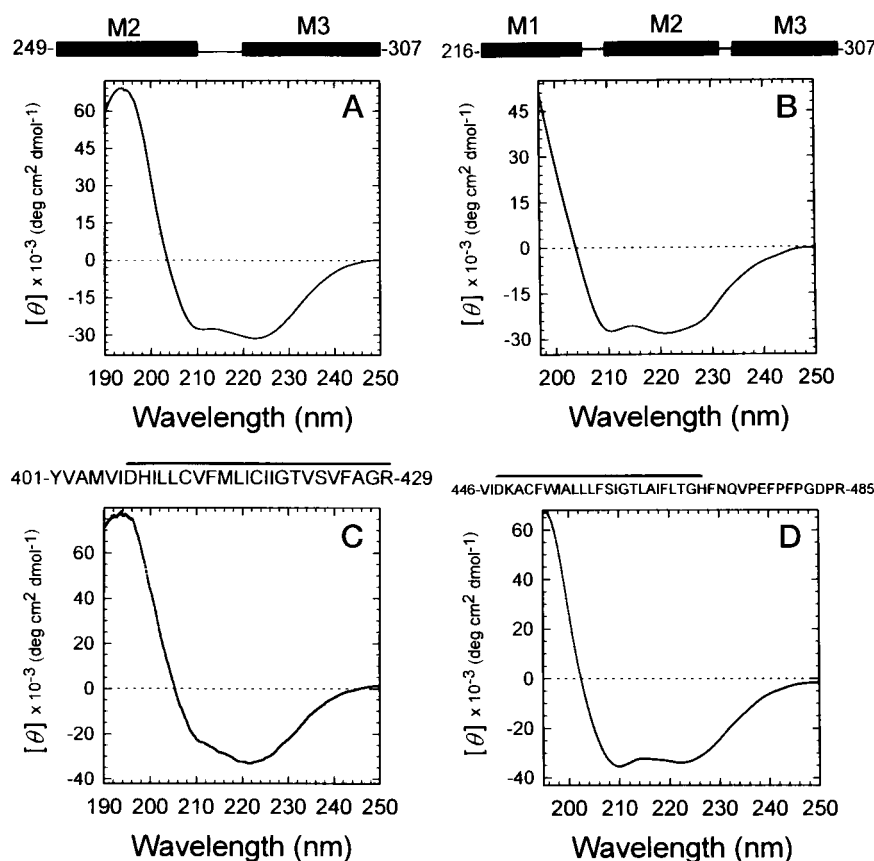


FIG. 2. CD spectra of peptide fragments  $\beta$ -T-8K,  $\beta$ -T-10K,  $\alpha$ -T-4K, and  $\gamma$ -T-5K. HPLC-purified fragments  $\beta$ -T-8K,  $\beta$ -T-10K,  $\alpha$ -T-4K, and  $\gamma$ -T-5K were reconstituted into lipid (asolectin) vesicles as described under "Experimental Procedures." CD spectra were measured for each reconstituted peptide (in 10 mM sodium phosphate, 5 mM sodium chloride buffer, pH 7.0). Panel A, CD spectrum of the  $\beta$ -subunit tryptic peptide  $\beta$ -T-8K (Met<sup>249</sup>-Arg<sup>307</sup>), which contains the transmembrane segments M2 and M3 ( $\sim 5 \mu\text{M}$ ). Panel B, CD spectrum of  $\beta$ -T-10K (Lys<sup>216</sup>-Arg<sup>307</sup>), which contains the transmembrane segments M1, M2, and M3 ( $\sim 0.35 \mu\text{M}$ ). Panel C, CD spectrum of  $\alpha$ -T-4K (Tyr<sup>401</sup>-Gly<sup>437</sup>), which contains the transmembrane segment M4 ( $\sim 5 \mu\text{M}$ ). Panel D, CD spectrum of  $\gamma$ -T-5K (Val<sup>446</sup>-Arg<sup>485</sup>), which contains the transmembrane segment M4 ( $\sim 5 \mu\text{M}$ ). Spectra were obtained by averaging over 5–10 scans with background subtracted.

TABLE I

## Summary of secondary structure results derived from CD spectra

Values for CD analysis were obtained by spectral deconvolution using the basis spectra of Chang *et al.* (31). Other indicates unordered/random structure and structures otherwise not assigned. Dash indicates the absence of a particular conformation in the secondary structure estimation.

	$\alpha$ -Helix	$\beta$ -Sheet	$\beta$ -Turn	Other
	%	%	%	%
$\beta$ -T-8K (M2-M3)	85	—	15	—
$\beta$ -T-10K (M1-M2-M3)	80	—	20	—
$\alpha$ -T-4K (M4)	87	—	13	—
$\gamma$ -T-5K (M4)	80	—	11	9

random coil. The strong intensity at  $1653 \text{ cm}^{-1}$  in  $^2\text{H}_2\text{O}$  further supports the predominantly  $\alpha$ -helical nature of the  $\gamma$ -M4 polypeptide. Similar spectral changes were observed upon transfer of the peptide  $\beta$ -T-8K ( $\beta$ -M2-M3) from  $^1\text{H}_2\text{O}$  to  $^2\text{H}_2\text{O}$ .

To quantify the relative amounts of secondary structure in both the transmembrane segments  $\gamma$ -M4 and  $\beta$ -M2-M3, the spectra were curve fit according to the procedure described by Méthot *et al.* (45). The resulting curve fit spectra are shown in Fig. 5 and the numerical secondary structure estimates presented in Table III. The curve fit data suggest a predominance of  $\alpha$ -helical secondary structure (65% and 75% for  $\gamma$ -M4 and  $\beta$ -M2-M3, respectively) in agreement with the qualitative analyses of the FTIR spectra. However, the curve fit may actually underestimate the percentage of  $\alpha$ -helices for two reasons. 1) Residual intensity remains in the amide II band near  $1547$

$\text{cm}^{-1}$  in both sets of spectra recorded in  $^2\text{H}_2\text{O}$  (data not shown), indicating that there are unexchanged peptide hydrogens. Although it is standard practice to fit the  $\alpha$ -helical band as one peak, the broad absorbance centered near  $1653 \text{ cm}^{-1}$  may actually contain unresolved vibrations due to both protonated and deuterated  $\alpha$ -helices. Curve fitting either spectra of  $\gamma$ -M4 or  $\beta$ -M2-M3 with two  $\alpha$ -helical bands due to protonated and deuterated  $\alpha$ -helices would likely increase the estimated proportion of  $\alpha$ -helices at the expense of random coil. 2) Deposition of the peptide-lipid bilayers on the planar surface of the ATR crystal should lead to planar orientation of the samples. The intrinsic dichroism of the ATR crystal will reduce slightly the intensity of vibrations oriented predominantly perpendicular to the ATR surface relative to those vibrations that are randomly oriented. This could lead to a slight reduction in the intensity of the  $\alpha$ -helical vibrations, as is observed in spectra of intact nAChR recorded using the ATR *versus* the transmission techniques (45, 46). Note we attributed the vibration near  $1627 \text{ cm}^{-1}$  to  $\beta$ -sheet. However, the  $\alpha$ -helical protein myoglobin absorbs in this region of the spectrum, despite a complete absence of  $\beta$ -strands. In addition, bands near this region have also been attributed to denatured and aggregated polypeptides (43). The conclusion that can thus be drawn from the FTIR studies is that both transmembrane fragments have a propensity to adopt an  $\alpha$ -helical conformation.

## DISCUSSION

The goal of the present work was to determine the secondary structure of peptide fragments of the nicotinic AChR that con-

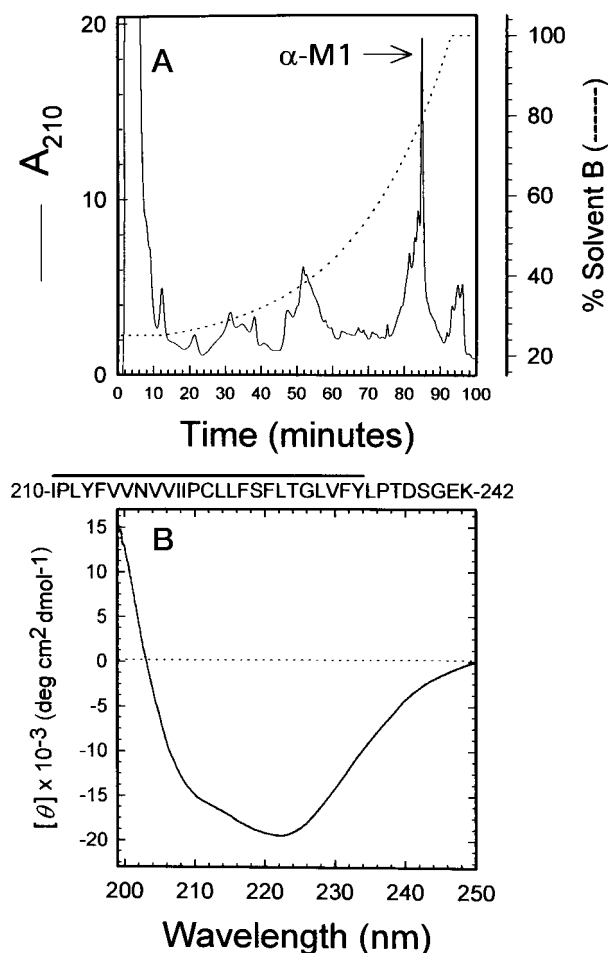


FIG. 3. Reverse-phase HPLC purification and CD spectra of the transmembrane fragment  $\alpha$ -M1. Panel A, AChR-rich membranes ( $\sim 50$  mg of protein) were resolved by SDS-PAGE and each of the AChR subunits isolated. For the  $\alpha$ -subunit,  $\alpha$ -V8-20 (Ser<sup>173</sup>-Glu<sup>338</sup>) was isolated from a limited "in gel" digest of the intact subunit (see "Experimental Procedures"). The  $\alpha$ -V8-20 fragment was then digested in solution with trypsin, and the digest resolved on 1.5-mm-thick 16.5% T, 6% C Tricine SDS-PAGE gels. The tryptic gel fragment  $\alpha$ -T-4K was isolated and further purified by reverse-phase HPLC (see Fig. 1 legend) with the elution of the peptide monitored by absorbance at 210 nm (solid line). The  $\alpha$ -T-4K fragment elutes at about 85 min (see arrow), and the fragment identity (Ile<sup>210</sup>-Lys<sup>216</sup>,  $\alpha$ -M1) was subsequently confirmed by NH<sub>2</sub>-terminal amino acid sequence analysis. Panel B, HPLC-purified fragment  $\alpha$ -T-4K ( $\alpha$ -M1) was reconstituted into lipid (asolectin) vesicles as described under "Experimental Procedures" and the CD spectrum measured (in 10 mM sodium phosphate, 5 mM sodium chloride buffer, pH 7.0). The  $\alpha$ -T-4K (10  $\mu$ M) peptide contains the transmembrane segment M1 of the  $\alpha$ -subunit, and the final CD spectrum was obtained by averaging over five scans with background subtracted.

TABLE II

Secondary structure analysis of the CD spectrum of  $\alpha$ -M1 peptide

Values for CD analysis were obtained by spectral deconvolution using the basis spectra of Chang *et al.* (31). Other indicates unordered/random structure and structures otherwise not assigned. Dash indicates the absence of a particular conformation in the secondary structure estimation.

	$\alpha$ -Helix	$\beta$ -Sheet	$\beta$ -Turn	Other
	%	%	%	%
$\alpha$ -T-4K (M1)	56	—	15	29

tained one or more membrane-spanning segments. The CD and FTIR results show that the membrane-bound AChR peptides ( $\beta$ -M2-M3,  $\beta$ -M1-M2-M3,  $\alpha$ -M4,  $\gamma$ -M4, and  $\alpha$ -M1) are all largely  $\alpha$ -helical. In each of the peptides, the majority of amino acid residues are contained within the hydrophobic stretch, which

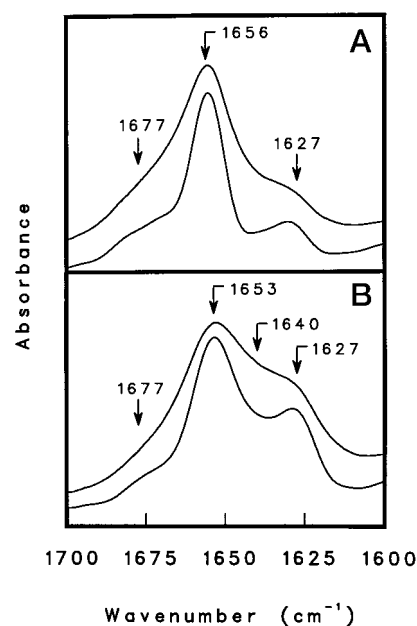


FIG. 4. Resolution-enhanced amide I band from FTIR spectra of the peptide fragment  $\gamma$ -T-5K ( $\gamma$ -M4) recorded in either <sup>1</sup>H<sub>2</sub>O (A) or <sup>2</sup>H<sub>2</sub>O (B) buffer. Each panel shows the absorbance (top curve) and deconvoluted (lower curve) spectra. Spectra parameters are described under "Experimental Procedures."

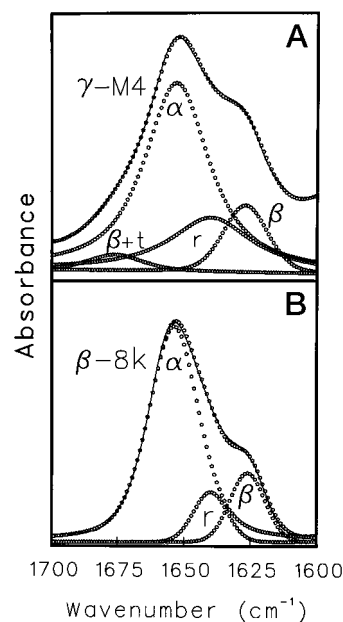


FIG. 5. Curve fit analysis of FTIR spectra (amide I region) recorded in <sup>2</sup>H<sub>2</sub>O of peptide fragments  $\gamma$ -T-5K (A) and  $\beta$ -T-8K (B). In each panel, the solid line represents the experimental data. The curve fit spectrum (dotted line) is superimposed onto the experimental spectrum. The best fit of individual component bands (dotted lines) are also presented.

constitutes the transmembrane segment. For example, in  $\alpha$ -M4 23 out of 29 residues (80%) are contained within the transmembrane segment M4; ( $\beta$ -M2-M3, 46/60, 77%;  $\beta$ -M1-M2-M3, 72/92, 77%;  $\gamma$ -M4, 24/40, 60%;  $\alpha$ -M1, 25/33, 75%). Therefore, the largely helical nature of each peptide is predominantly a reflection of the secondary structure of the membrane-spanning domain. The polytopic or multispanning membrane protein bacteriorhodopsin provides an example in which the structure of isolated transmembrane segments/peptides has been shown to retain the  $\alpha$ -helical structure observed in the high resolution

TABLE III

Summary of secondary structure results derived from FTIR spectra

Values for FTIR analysis were obtained using the curve-fitting routine (GRAMS/386 version 1, Galactic Industries, Salem, NH) and according to the procedure described by Méthot *et al.* (45). Dash indicates the absence of a particular conformation in the secondary structure estimation.

	$\alpha$ -Helix	$\beta$ -Sheet	$\beta$ -Sheet + turn	Random
	%	%	%	%
$\beta$ -T-8K (M2-M3)	75	15	—	10
$\gamma$ -T-5K (M4)	65	12	3	20

three-dimensional structure of the intact protein (see, *e.g.*, Ref. 40). Nonetheless, it should be noted that the secondary structure of isolated peptides containing transmembrane segments of the AChR may not necessarily reflect the structure found in the intact receptor. Although, as is discussed in more detail below, the present spectroscopic results are consistent with the results of structural studies done with the intact AChR, a definitive answer as to whether isolated lipid-reconstituted AChR peptides retain the structure found in the intact protein remains to be established.

A wealth of information has accumulated pointing to the  $\alpha$ -helical nature of the AChR M2 domain (reviewed in Ref. 47). These studies include such diverse approaches as cryoelectron microscopy (10), examining the labeling pattern of photoreactive noncompetitive antagonists (34), to CD and NMR spectroscopy of synthetic channel-forming peptides (48, 49). In the present study, the largely  $\alpha$ -helical structure of the peptides  $\beta$ -M2-M3 and  $\beta$ -M1-M2-M3 indicate that the M3 and M1 domains are also likely  $\alpha$ -helical. Although considerably fewer studies have focused on the structure of the transmembrane segments M1, M3, and M4, for the most part those studies are in agreement with the present spectroscopic results. For example, the structure of the M3 segment in the intact AChR has been examined using different lipophilic photoreactive probes (21, 22). For the M3 segment of each AChR subunit, the pattern of incorporation was consistent with that of an  $\alpha$ -helix with the labeled residues situated on a common face, extending three or four turns of the helix. In a similar fashion, the M4 segment of each receptor subunit was also determined to be  $\alpha$ -helical (20–23). In contrast, as is discussed in more detail below, the structure of the M1 domain was not readily apparent from the few structural studies that have been conducted.

Although deconvolution of the CD spectrum of  $\alpha$ -M1 (Fig. 3B, Table II) indicates that the peptide is largely  $\alpha$ -helical, there is also a substantial amount of non-helical structure present ( $\alpha$ -helix = 56%,  $\beta$ -turn = 15%, random = 29%). Similar results were obtained from the CD spectrum of a synthetic peptide containing the M1 domain of the AChR  $\delta$ -subunit ( $\alpha$ -helix = 60%,  $\beta$ -sheet = 19%,  $\beta$ -turn = 21%; see Ref. 48). A unique feature of the M1 domain is that it contains three proline residues including a highly conserved proline (*i.e.*  $\alpha$ -Pro<sup>221</sup>) in the middle of the domain. Among globular proteins the proline residue is considered the classic helix-breaker (50). The proline nitrogen lacks a proton so that the peptide bond cannot participate in hydrogen bonding to a neighboring carbonyl group within the helix. It is then somewhat surprising that proline residues are found frequently in the putative transmembrane domains of many integral membrane proteins, including the  $\alpha$ -helical segments of bacteriorhodopsin (51), the photosynthetic reaction center (52), and aquaporin (53, 54). In contrast, proline is excluded from the core of the  $\beta$ -barrel transmembrane region of bacterial porins, an observation that is consistent with its ability to also act effectively as a  $\beta$ -sheet breaker (55). A proline residue introduces a kink in the backbone of an  $\alpha$ -helix (56), and this distortion may account for the deviation

in the M1 CD spectrum from that of a more classical  $\alpha$ -helix (57). The presence of two proline residues in the extracellular half of  $\alpha$ -M1 might also explain the irregular structure deduced for this region in a recent report from Akabas & Karlin (58). The authors found that several residues in the amino-terminal half of  $\alpha$ -M1 (between Pro<sup>211</sup> and Pro<sup>221</sup>) when mutated to cysteine are accessible to hydrophilic sulfhydryl reagents. The pattern of accessibility suggested an unordered structure for this region (see also Ref. 59). An alternative explanation is that distortions in the helical backbone introduced by Pro<sup>211</sup> and Pro<sup>221</sup> might alter the exposure of surrounding residues to these hydrophilic sulfhydryl reagents. It is also important to point out that the hydrophilic sulfhydryl reagents are presumed to access residues in  $\alpha$ -M1 from the aqueous lumen of the ion channel, suggesting that these residues are exposed to the channel pore. In contrast, from the pattern of labeling by the hydrophobic reagent [<sup>125</sup>I]TID, Blanton and Cohen (21) concluded that residues in the COOH-terminal half of  $\alpha$ -M1 are exposed to the lipid bilayer. Interestingly, the pattern of [<sup>125</sup>I]TID incorporation into  $\alpha$ -M1 was like the sulfhydryl reagent neither consistent with that of an  $\alpha$ -helix or a  $\beta$ -sheet. The hydrophobic labeling pattern might also be a consequence of the presence of proline residues within  $\alpha$ -M1 (Pro<sup>221</sup> and Pro<sup>236</sup>). Alternatively, the membrane-spanning segment ( $\alpha$ -M1) might contain sections that adopt an unordered or irregular secondary structure. Given the functional importance of the M1 domain (60, 61), further structural examination is clearly warranted.

Finally, the residual non-helical structures estimated from deconvolution of the CD spectra of most of the AChR transmembrane peptides, the exception being  $\alpha$ -M1, is largely estimated as being  $\beta$ -turn (Table I). Turn structure is consistent with the presence of residues in each peptide that contribute to the loops connecting each of the membrane-spanning segments, in particular the short loops joining M1-M2-M3. The presence of  $\beta$ -turn is also consistent with what appears to be a consensus loop structure connecting the transmembrane segments of integral membrane proteins (62).

## CONCLUSION

In this paper, we have combined CD and ATR-FTIR spectroscopy to determine the structure of peptides that contain one or more transmembrane domains of the nicotinic AChR. The spectroscopic results demonstrate that the isolated membrane-spanning domains M1, M2, M3, and M4 all adopt a largely  $\alpha$ -helical conformation. These studies provide additional support for reports (20, 21, 24) that conclude that the transmembrane region of the AChR comprises predominantly, if not exclusively, of bundles of membrane-spanning  $\alpha$ -helices. These studies also represent the first step of a possible approach for examining in detail the nature of the interactions between transmembrane segments and specific lipids that are required for receptor function. Finally, by further examining the structure of peptides containing one, two, and three or more transmembrane domains, insight into the nature of inter-domain interactions may be achieved.

*Acknowledgment*—We thank Dr. Anthony Fink for kindly allowing us use of his AVIV 60DS CD spectropolarimeter.

## REFERENCES

- Reynolds, J. A., and Karlin, A. (1978) *Biochemistry* **17**, 2035–2038
- Raftery, M. A., Hunkapiller, M. W., Stader, C. D., and Hood, L. E. (1980) *Science* **208**, 1454–1457
- Hucho, F., Tsetlin, V. I., and Machold, J. (1996) *Eur. J. Biochem.* **239**, 539–557
- Karlin, A., and Akabas, M. H. (1995) *Neuron* **15**, 1231–1244
- Smith, G. B., and Olsen, R. W. (1995) *Trends Pharmacol. Sci.* **16**, 162–168
- Jackson, M. B., and Yakel, J. L. (1995) *Annu. Rev. Physiol.* **57**, 447–68
- Kuhse, J., Betz, H., and Kirsch, J. (1995) *Curr. Opin. Neurobiol.* **5**, 318–323
- Mitra, A. K., McCarthy, M. P., and Stroud, R. M. (1989) *J. Cell Biol.* **109**,

755-774

9. Toyoshima, C., and Unwin, N. (1990) *J. Cell Biol.* **111**, 2623-2635
10. Unwin, N. (1993) *J. Mol. Biol.* **229**, 1101-1124
11. Noda, M., Takahashi, H., Tanabe, T., Toyosato, M., Furutani, Y., Hirose, T., Asai, M., Inayama, S., Miyata, T., and Numa, S. (1982) *Nature* **299**, 793-797
12. Noda, M., Takahashi, H., Tanabe, T., Toyosato, M., Kikuyotani, S., Hirose, T., Asai, M., Takashima, H., Inayama, S., Miyata, T., and Numa, S. (1983) *Nature* **301**, 251-255
13. Noda, M., Takahashi, H., Tanabe, T., Toyosato, M., Kikuyotani, S., Furutani, Y., Hirose, T., Takashima, H., Inayama, S., Miyata, T., and Numa, S. (1983) *Nature* **302**, 528-532
14. Claudio, T., Ballivet, M., Patrick, J., and Heinemann, S. (1983) *Proc. Natl. Acad. Sci. U. S. A.* **80**, 1111-1115
15. Cont-Tronconi, B. M., McLane, K. E., Raftery, M. A., Grando, S. A., Protti, M. P. (1994) *Crit. Rev. Biochem. Mol. Biol.* **29**, 69-123
16. Unwin, N. (1995) *Nature* **373**, 37-43
17. Changeux, J. P., Galzi, J.-L., Devillers-Thierry, A., and Bertrand, D. (1992) *Q. Rev. Biophys.* **25**, 395-432
18. Karlin, A. (1993) *Curr. Opin. Neurobiol.* **3**, 299-309
19. Gorne-Tschelnokow, U., Strecker, A., Kaduk, C., Naumann, D., and Hucho, F. (1994) *EMBO J.* **13**, 338-341
20. Blanton, M. P., and Cohen, J. B. (1992) *Biochemistry* **31**, 3738-3750
21. Blanton, M. P., and Cohen, J. B. (1994) *Biochemistry* **33**, 2859-2872
22. Blanton, M. P., Dangott, L. J., Raja, S. K., Lala, A. K., and Cohen, J. B. (1995) *Biophys. J.* **68**, A377 (abstr.)
23. Blanton, M. P., Dangott, L. J., Xie, Y., and Cohen, J. B. (1997) *Biophys. J.* **72**, 152a (abstr.)
24. Baenziger, J. E., and Méthot, N. (1995) *J. Biol. Chem.* **270**, 29129-29137
25. Sobel, A., Weber, M., and Changeux, J. P. (1977) *Eur. J. Biochem.* **80**, 215-224
26. Pedersen, S. E., Dreyer, E. B., and Cohen, J. B. (1986) *J. Biol. Chem.* **261**, 13735-13743
27. Laemmli, U. K. (1970) *Nature* **227**, 680-685
28. Cleveland, D. W., Fischer, S. G., Kirschner, M. W., and Laemmli, U. K. (1977) *J. Biol. Chem.* **252**, 1102-1106
29. Hager, D. A., and Burgess, R. R. (1980) *Anal. Biochem.* **109**, 76-86
30. Schagger, H., and von Jagow, G. (1987) *Anal. Biochem.* **166**, 368-379
31. Chang, C. T., Wu, C.-S. C., and Yang, J. T. (1978) *Anal. Biochem.* **91**, 13-31
32. Reid, S. E., Moffatt, D. J., and Baenziger, J. E. (1996) *Spectrochim. Acta* **52**, 1347-1356
33. Pedersen, S. E., Sharp, S. D., Liu, W. S., and Cohen, J. B. (1992) *J. Biol. Chem.* **267**, 10489-10499
34. White, B. H., and Cohen, J. B. (1992) *J. Biol. Chem.* **267**, 15770-15783
35. Greenfield, N. J. (1996) *Anal. Biochem.* **235**, 1-10
36. Kelly, S. M., and Price, N. C. (1997) *Biochim. Biophys. Acta* **1338**, 161-185
37. Park, K., Perczel, A., and Fasman, G. D. (1992) *Protein Sci.* **1**, 1032-1049
38. Li, S. C., and Deber, C. M. (1992) *Int. J. Peptide Protein Res.* **40**, 243-248
39. Henry, G. D., and Sykes, B. D. (1994) *Methods Enzymol.* **239**, 515-535
40. Ozawa, S., Hayashi, R., Masuda, A., Iio, T., and Takahashi, S. (1997) *Biochim. Biophys. Acta* **1323**, 145-153
41. Lomize, A. L., Pervushin, K. V., and Arseniev, A. S. (1992) *J. Biomol. NMR* **2**, 361-372
42. Waterhous, D. V., and Johnson, W. C., Jr. (1994) *Biochemistry* **33**, 2121-2128
43. Jackson, M., and Mantsch, H. H. (1995) *Crit. Rev. Biochem. Mol. Biol.* **30**, 95-120
44. Baenziger, J. E., and Chew, J. E. (1997) *Biochemistry* **36**, 3617-3624
45. Méthot, N., McCarthy, M. P., and Baenziger, J. E. (1994) *Biochemistry* **33**, 7709-7717
46. Méthot, N., Demers, C. N., and Baenziger, J. E. (1995) *Biochemistry* **34**, 15142-15149
47. Galzi, J. L., and Changeux, J. P. (1995) *Neuropharmacology* **34**, 563-582
48. Montal, M., Montal, M. S., and Tomich, J. M. (1990) *Proc. Natl. Acad. Sci. U. S. A.* **87**, 6929-6933
49. Bechinger, B., Kim, Y., Chirlan, L. E., Gesell, J., Neumann, J., Montal, M., Tomich, J., Zasloff, M., and Opella, S. J. (1991) *J. Biomol. NMR* **1**, 167-173
50. Chou, P. Y., and Fasman, G. D. (1978) *Annu. Rev. Biochem.* **47**, 251-257
51. Henderson, R., Baldwin, J. M., Ceska, T. A., Zemlin, F., Beckman, E., and Downing, K. M. (1990) *J. Mol. Biol.* **213**, 899-929
52. Deisenhofer, J., Epp, O., Miki, K., Huber, R., and Michel, H. (1985) *Nature* **318**, 618-624
53. Walz, T., Hirai, T., Murata, K., Heymann, J. B., Mitsuoka, K., Fujiyoshi, Y., Smith, B. L., Agre, P., and Engel, A. (1997) *Nature* **387**, 624-627
54. Cheng, A., van Hoek, A. N., Yeager, M., Verkman, A. S., and Mitra, A. K. (1997) *Nature* **387**, 627-630
55. Li, S. C., Goto, N., Williams, K. A., and Deber, C. M. (1996) *Proc. Natl. Acad. Sci.* **93**, 6676-6681
56. von Heijne, G. (1991) *J. Mol. Biol.* **218**, 499-503
57. Li, S. C., Deber, C. M., and Shoelson, S. E. (1994) *Biochemistry* **33**, 14333-14338
58. Akabas, M. H., and Karlin, A. (1995) *Biochemistry* **34**, 12496-12500
59. Tamamizu, S., Todd, A. P., and McNamee, M. G. (1995) *Cell. Mol. Neurobiol.* **15**, 427-438
60. Tobimatsu, T., Fujita, Y., Fukuda, K., Tanaka, K.-I., Mori, Y., Konno, T., Mishina, M., and Numa, S. (1987) *FEBS Lett.* **222**, 56-62
61. Wang, H.-L., Auerbach, A., Bren, N., Ohno, K., Engel, A. G., and Sine, S. M. (1997) *J. Gen. Physiol.* **109**, 757-766
62. Yeagle, P. L., Alderfer, J. L., Salloum, A. C., Ali, L., and Albert, A. D. *Biochemistry* **36**, 3864-3869